INVESTIGATION OF ROTATING FLOWS WITH SEPARATION USING THE ELLIPTIC-BLENDING REYNOLDS-STRESS MODEL

Rémi Manceau

Departement of applied mathematics
CNRS–University of Pau and Inria-CAGIRE group
IPRA, avenue de l'université, 64013 Pau, France
remi.manceau@univ-pau.fr

ABSTRACT

The present paper addresses the issue of the reproduction of rotating flows with separation of the boundary layer that are relevant to many turbomachinery applications. In order to account for both the wall/turbulence and the Coriolis force/turbulence interactions at the RANS level, a second-moment closure valid in the near-wall region is necessary. The Elliptic Blending Reynolds Stress Model (EB-RSM), originally proposed by Manceau & Hanjalić (2002) is such a closure model. Various modifications to this model by several authors during the last decade are revisited from the theoretical standpoint and investigated in detail in comparison with recent DNS databases for high-Reynolds number channel flows, spanwise rotating channel flows with strong rotation rates, up to complete laminarization, and the separated flow after a sudden expansion without and with system rotation.

INTRODUCTION

Rotating flows are of considerable importance to many industrial fields, in particular turbomachinery, or in geophysical and astrophysical applications. These flows are moreover very challenging for turbulence models (see, for instance, the review of Jakirlić *et al.*, 2002). In particular, internal flows with spanwise rotation are relevant to the flow in turbine blade passages, in which Coriolis forces yield a strong modification of the Reynolds stresses, which in turn have a significant impact on the mean velocity field. This type of flows is thus particularly relevant to the evaluation of the performance of a turbulence model.

The present study aims at reproducing the case of a channel flow with sudden expansion under spanwise rotation, corresponding to the very recent DNS data of Lamballais (2014). This geometrically simple configuration is relevant to the study of the influence of rotation on separated regions, which is often encountered in turbomachinery applications. Despite their challenging character for turbulence models and its practical importance, this configuration has been the subject of only very few experimental (Rothe & Johnston, 1979; Visscher & Andersson, 2011), DNS (Barri & Andersson, 2010; Lamballais, 2014), and turbulence modeling (Iaccarino *et al.*, 1999; Viswanathan & Tafti, 2007) studies. To the knowledge of the author, sudden-expansion flows with spanwise rotation have never been investigated with second moment closures.

The Elliptic Blending Reynolds Stress Model (EB-RSM), originally proposed by Manceau & Hanjalić (2002) to extend standard, weakly inhomogeneous Reynolds stress models to the near-wall region, has been subject to various modifications by

several authors during the last decade, mainly for numerical robustness reasons. Indeed, the first applications of the Elliptic Blending strategy to complex configurations highlighted some deficiencies of the model, which is at the origin of various modifications that mainly affect the formulations for the velocity–pressure gradient tensor, the blending function used to migrate from the near-wall form to the weakly inhomogeneous form of the model and the dissipation equation. On the one hand, such a variability is evidence that the model is alive and applied to practical configurations, but, on the other hand, it is a source of confusion, since the appellation *Elliptic Blending Reynolds Stress Model* (EB-RSM) actually refers to numerous, slightly different models.

Therefore, during the course of the present study, all these modifications have been revisited, with the objective of accurately reproducing rotating flows and preserving the numerical robustness. The analysis exploits recent DNS databases for high-Reynolds number channel flows, spanwise rotating channel flows with strong rotation rates, up to complete laminarization, and the separated flow after a sudden expansion without and with system rotation. Some of these databases have not been exploited yet in the context of RANS modeling (Lozano-Durán & Jiménez, 2014; Lamballais, 2014).

THE ELLIPTIC-BLENDING REYNOLDS-STRESS MODEL (EB-RSM)

The Reynolds-stress transport equation reads

$$\frac{\mathrm{D}\overline{u_i u_j}}{\mathrm{D}t} = P_{ij} + G_{ij} + D_{ij}^{\nu} + D_{ij}^{T} + \phi_{ij}^{*} - \varepsilon_{ij}, \qquad (1)$$

where $\mathbf{P}$, $\mathbf{D^\nu}$, $\mathbf{D^T}$, Φ^* and $\mathbf{E}$ stand for the production, the molecular diffusion, the turbulent diffusion, the velocity-pressure gradient correlation and the dissipation tensors, respectively. $G_{ij} = -2\omega_k(\varepsilon_{ikm}\overline{u_j u_m} + \varepsilon_{jkm}\overline{u_i u_m})$ is the redistribution term arising from the Coriolis acceleration, where ω is the rotation axial vector.

The main specificity of the EB-RSM is the modeling of the difference $\Phi^* - \mathbf{E}$ as a blending

$$\Phi^* - \mathbf{E} = (1-f)(\Phi^w - \mathbf{E}^w) + f(\Phi^h - \mathbf{E}^h), \qquad (2)$$

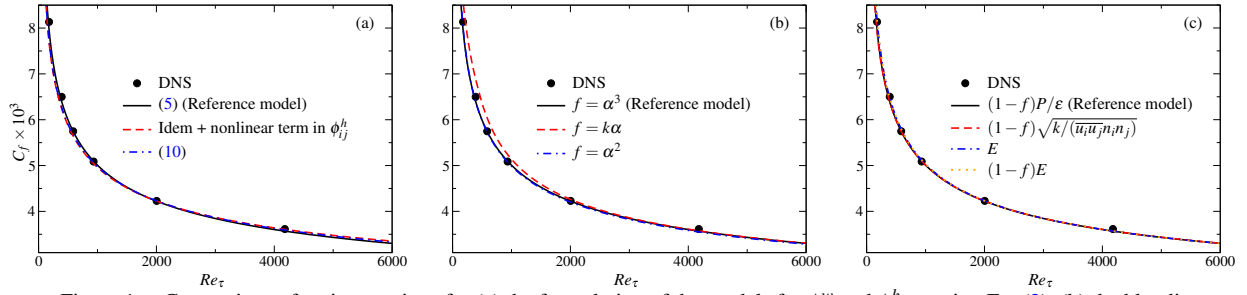of a standard model, herein the SSG model (Speziale *et al.*,

Figure 1. Comparison of various options for (a) the formulation of the models for ϕ_{ij}^w and ϕ_{ij}^h entering Eq. (2); (b) the blending function f entering Eq. (2); (c) The additional production term in the ε-equation. Comparisons are performed in a channel flow for 90 different imposed values of Re_τ ranging from 100 to 6000.

1991),

$$\Phi^h - \mathbf{E}^h = -\left(g_1 + g_1^* \frac{P}{\varepsilon}\right)\varepsilon\mathbf{b} + g_2\varepsilon\left(\mathbf{b}^2 - \frac{1}{3}\{\mathbf{b}^2\}\mathbf{I}\right)$$
$$+\left(g_3 - g_3^*\sqrt{\{\mathbf{b}^2\}}\right)k\mathbf{S} + g_4k\left(\mathbf{bS} + \mathbf{Sb} - \frac{2}{3}\{\mathbf{bS}\}\mathbf{I}\right)$$
$$+g_5k\left(\mathbf{bW} + \mathbf{Wb}\right) - \frac{2}{3}\varepsilon\mathbf{I}, \qquad (3)$$

where $\mathbf{b}$, $\mathbf{S}$ and $\mathbf{W}$ are the anisotropy, mean strain and absolute rotation tensors, respectively; and the near-wall model given by

$$\frac{\Phi^w - \mathbf{E}^w}{\varepsilon} = -\frac{2}{3}\mathbf{I} + a_1\mathbf{b} + a_2\left(1 + a_2'\{\mathbf{bM}\}\right)\mathbf{M}$$
$$+a_3\left(\mathbf{bM} + \mathbf{Mb} - \frac{2}{3}\{\mathbf{bM}\}\mathbf{I}\right), \qquad (4)$$

where

$$a_1 = -\frac{26}{3}; \; a_2 = -5; \; a_2' = -1; \; a_3 = -10, \qquad (5)$$

and $\mathbf{M} = \mathbf{n} \otimes \mathbf{n} - \frac{1}{3}\mathbf{I}$. The blending function $f = \alpha^3$ is related to the distance-to-the-wall-sensitive function α, solution of the elliptic relaxation equation:

$$\alpha - L^2\nabla^2\alpha = 1. \qquad (6)$$

that ranges from 0 at the wall to 1 far from the wall. The unit vector $\mathbf{n}$ is a generalization of the notion of wall-normal vector: $\mathbf{n} = \nabla\alpha/\|\nabla\alpha\|$.

In the dissipation equation,

$$\frac{\mathrm{D}\varepsilon}{\mathrm{D}t} = \frac{C_{\varepsilon_1}'P - C_{\varepsilon_2}\varepsilon}{T} + \frac{\partial}{\partial x_l}\left(\frac{C_\mu}{\sigma_\varepsilon}\overline{u_l u_m}T\frac{\partial\varepsilon}{\partial x_m}\right) + \nu\frac{\partial^2\varepsilon}{\partial x_k\partial x_k} + E, \; (7)$$

the term

$$E = C_{\varepsilon 3}\nu\frac{k}{\varepsilon}\overline{u_j u_k}\left(\frac{\partial^2 U_i}{\partial x_j\partial x_l}\right)\left(\frac{\partial^2 U_i}{\partial x_k\partial x_l}\right) \qquad (8)$$

is intended to represent the term $P_{\varepsilon 3}$ in the exact ε-equation (Hanjalić & Launder, 2011), which peaks in the buffer layer, and is negligible in weakly inhomogeneous regions
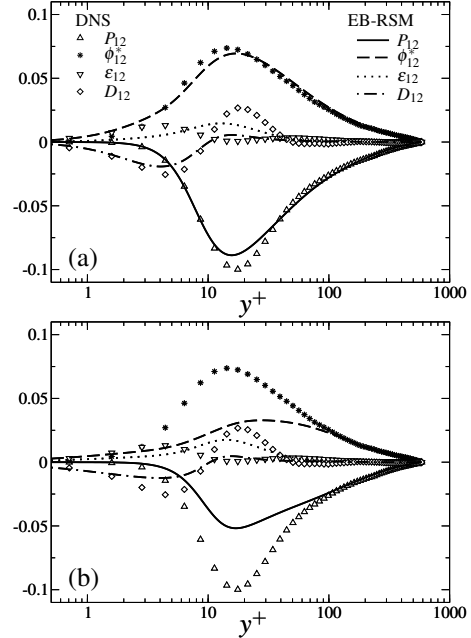

Figure 2. Computation of a channel flow at $Re_\tau = 590$. Budget of the $\overline{uv}$ component. Comparison of the formulations (a) Eq. (5) and (b) Eq. (10).

(Mansour et al., 1988), such that it is usually not accounted for in standard models. In order to avoid numerical difficulties linked to the term E, this term is replaced ($C_{\varepsilon 3} = 0$) by a variable $C_{\varepsilon 1}'$ coefficient that stimulates the production of dissipation in the buffer layer

$$C_{\varepsilon_1}' = C_{\varepsilon_1}\left[1 + A_1\left(1 - f\right)\frac{P}{\varepsilon}\right]. \qquad (9)$$

The equations above constitute the *reference model*.

COMPARISON OF DIFFERENT VERSIONS OF THE EB-RSM

Starting from its proposal by Manceau & Hanjalić (2002), the model was subject to numerous modifications by several authors, in order to improve numerical stability and/or to improve the predictions for particular type of applications. These variability of the model is a source of confusion for new users, and, above all, some modifications have not been validated in simple, generic configurations. The purpose of the present section

2

is to clarify this issue by comparing the different formulations using theoretical and practical arguments, in order to select a recommended version of the model. This analysis is summarized below, the interested reader is referred to Manceau (2015).

(i) The inclusion or not of the nonlinear term in the slow part of the pressure-strain correlation does not have a significant influence on the results, in channel flows without (Fig. 1a) and with rotation (Fig. 3). The use of this term is consequently not recommended, for numerical stability reasons, although its influence in more general configuration should be investigated in the future.

(ii) In the original model, the near-wall formulation $\Phi^w - \mathbf{E}^w$ (4) with coefficients (5) does not lead to the correct asymptotic behavior of the components $\overline{uv}$ and $\overline{vw}$, where v is the wall-normal fluctuating velocity. The alternative formulation that corrects this behavior writes

$$a_1 = -\frac{14}{3}; \ a_2 = -5; \ a_2' = \frac{7}{5}; \ a_3 = -4 \quad (10)$$

(see Manceau, 2015). This formulation, which was used by Törnblom & Johansson (2007), yields virtually the same predictions as the original formulation (Fig. 1a), but does not give a correct prediction of the budgets of these Reynolds stress components (Fig. 2). In contrast, the standard formulation very satisfactorily reproduces these budgets, in non-rotating (Fig. 2) and rotating channel flows (Fig. 5), and is definitely recommended.

(iii) The original formulation of the blending function $f = k\alpha$ does not satisfactorily reproduce the friction coefficient in a channel flow over the range of friction Reynolds numbers for which DNS data are available (Fig. 1b) and does not behave correctly in rotating channels (Fig. 3). The formulations $f = \alpha^2$, proposed by Manceau (2003) and $f = \alpha^3$, proposed by Lecocq et al. (2008), yield very similar results (Fig. 1b and Fig. 3), and the latter is preferred based on the theoretical argument that it satisfies the exact asymptotic behavior of the crucial term $\phi_{22}^* - \varepsilon_{22}$ (Manceau, 2015).

(iv) The various formulations used to account for the $P_{\varepsilon 3}$ term in the exact dissipation equation yield very similar results in non-rotating (Fig. 1c) and rotating channel flows (Fig. 3) if coefficients are properly calibrated. The version using the variable coefficient (9) and $C_{\varepsilon 3} = 0$ is preferred to favor numerical robustness.

These conclusions have led to the formulation of the *reference* EB-RSM described in the previous section, in which $f = \alpha^3$ in Eq. (2), $g_2 = 0$ in Eq. (3), coefficients (5) are used in Eq. (4) and the production term $P_{\varepsilon 3}$ in the exact ε-equation is not represented by the term E, Eq. (8), but by the variable coefficient (9).

SPANWISE ROTATING CHANNEL FLOW

The performance of the reference model is investigated in cases with spanwise rotation, without (present section) and with separation (next section). Theoretical arguments (Manceau, 2015) show that the model does not require any adaptation to rotation in addition to the standard inclusion of the Coriolis redistribution term G_{ij} in Eq. (1) and the replacement of the mean vorticity tensor by the absolute mean vorticity tensor.

In spanwise rotating channel flows, the model correctly reproduces the effects of rotation (Fig. 3), in particular on the anticyclonic (pressure) side, but shows an inaccurate sensitivity
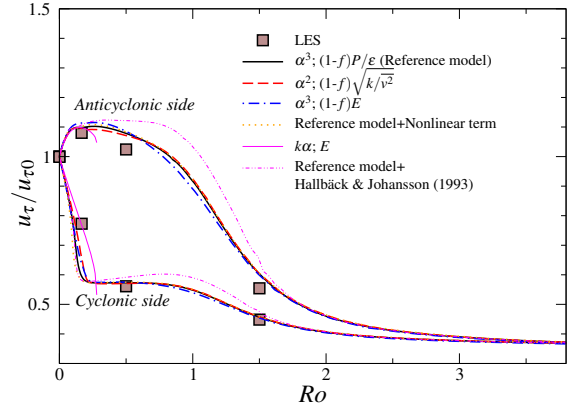

Figure 3. Rotating channel flows at $Re_b = 7000$. Ratio of the friction velocity u_τ to the friction velocity for the non-rotating case $u_{\tau 0}$. Comparison with the LES data of Lamballais et al. (1998).
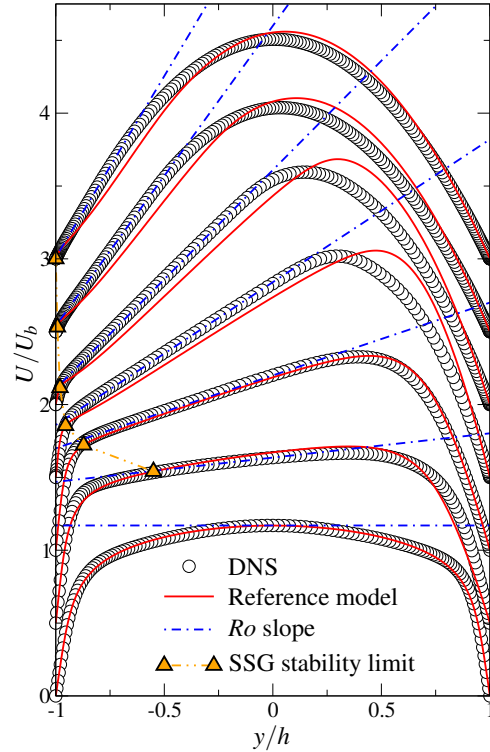

Figure 4. Rotating channel flow. Evolution with the rotation number of the mean velocity profile. Comparisons with the DNS data of Lamballais et al. (1998) at $Re_b = 2500$ for $Ro = 0$, 1/6 and 0.5 and with the DNS data of Grundestam et al. (2008) at $Re_\tau = 180$ for $Ro = 0.98$, 1.50, 2.06 and 2.49. Profiles are shifted for clarity.

to rotation on the cyclonic (suction) side (Fig. 4). Although many of the good properties of the model in rotating cases are to be attributed to the SSG model on which it relies far from the wall, the Elliptic Blending strategy appears relevant to extend this model to near-wall regions. In particular, the model gives a satisfactory, albeit not perfect, reproduction of the budgets of the Reynolds stresses, as shown in Fig. 5 (for a complete comparison, see Manceau, 2015).
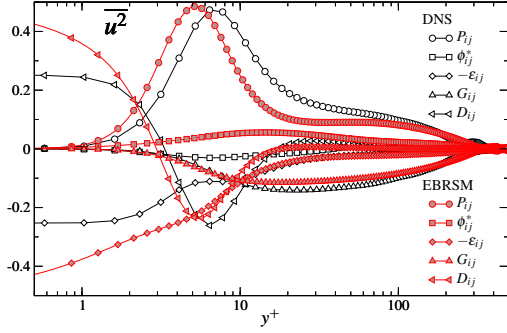
3

Figure 5. Budgets at $Re_\tau = 180$ of $\overline{u^2}$ in a channel flow with rotation number $Ro = 0.98$. Comparison with the DNS data Grundestam *et al.* (2008).

As a corollary, some discrepancies between the EB-RSM and DNS results are also inherited from the SSG model, in particular the slight under-prediction of the slope of the linear velocity profile in the core region and the delayed laminarization at high rotation numbers, which are linked to the slight over-prediction of the bifurcation threshold $\omega/S = 0.5$ for sheared homogeneous turbulence with system rotation (Fig. 4).

In Fig. 3, it is observed that the model is slightly over-sensitive to rotation for weak rotation numbers, on both sides of the channel. Moreover, on the anticyclonic side, after the maximal friction velocity is reached, the laminarization is too slow. In order to investigate possible improvement of these predictions, modifications of the dissipation equation are tested. Indeed, Bardina *et al.* (1983) emphasized the necessity of making the ε-equation sensitive to rotation, in order to account for the retardation of the energy cascade (Jacquin *et al.*, 1990; Sagaut & Cambon, 2008) and many modifications were proposed in the literature (for a recent review, see Jakirlić *et al.*, 2002). Here, four modifications, proposed by Bardina *et al.* (1985), Hallbäck & Johansson (1993), Shimomura (1993) and Rubinstein & Zhou (1997), respectively, were introduced in order to investigate their influence of the prediction of the friction velocities shown in Fig. 3. All these modifications aim at reducing the dissipation rate in rotating cases by increasing the destruction term in its transport equation, and yield similar incorrect results in the present case. To illustrate the effect of such terms, the results obtained with the modification of Hallbäck & Johansson (1993), which consists in sensitizing the destruction term of ε to the rotation rate by multiplying the $C_{\varepsilon 2}$ coefficient by the factor

$$1 + \frac{A\sqrt{Re_t}}{C_{\varepsilon 2}(25 + 2\omega^*)}\omega^* \qquad (11)$$

where Re_t is the turbulent Reynolds number $Re_t = k^2/(\nu\varepsilon)$ and $\omega^* = \omega k/\varepsilon$, are shown in Fig. 3. It can be seen that this modification has a dramatic effect on the results: the recommended coefficient $A = 0.6$ had to be reduced here to 0.1 to avoid a rapid departure from a physically admissible behavior. Moreover, the introduction of this term does not improve the results: for small values of Ro, the term has the undesired effect of increasing the sensitivity of the model to rotation; for large values of Ro, the laminarization is delayed, on both sides of the channel. Such modifications are intended to reproduce the effect of the inhibi-
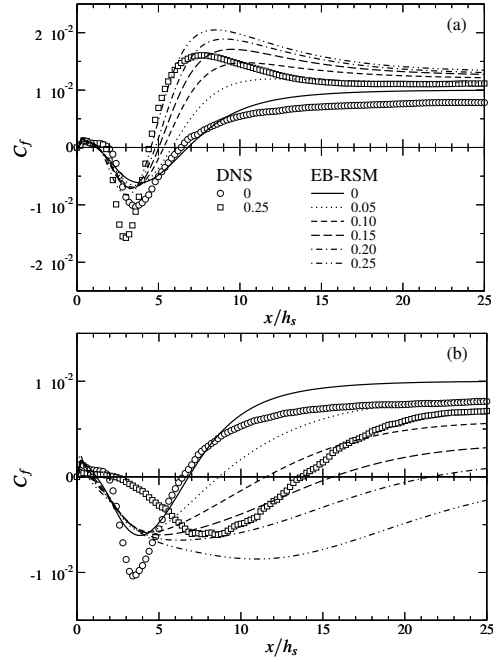

Figure 7. Channel with sudden expansion. Evolution with the rotation number of the C_f distribution after the expansion. (a) Anticyclonic side; (b) Cyclonic side.

tion of the energy cascade in homogeneous turbulence, and the present results suggest that they are not adequate for improving the results of the EB-RSM in wall-bounded, rotating, flows. Moderating the sensitivity of the model to rotation at low rotation rates and accelerating the laminarization at high rotation rates thus remains an open issue.

ROTATING CHANNEL FLOW WITH SUDDEN EXPANSION

The configuration of the rotating channel flow with sudden expansion is described in Fig. 6. This case is characterized by three non-dimensional numbers, chosen to match the configuration of Lamballais (2014): the expansion ratio $E_r = H/h = 3/2$; the Reynolds number $Re = hU_h/\nu = HU_H/\nu = 5000$; and the rotation number $Ro = 2\omega H/U_H = 0$ and 0.25. In addition, in order to better describe the evolution of the flow with the rotation rate, four intermediate rotation numbers are computed: $Ro = 0.05, 0.10, 0.15$ and 0.20.

Computations are performed with the open-source CFD solver *Code_Saturne*, developed by EDF (Archambeau *et al.*, 2004), based on the finite volume method in cell-centered collocated arrangement, using a second-order upwind-biased differencing scheme. Inlet boundary conditions are generated by a precursor computation in a fully-developed (periodic) channel flow, consistent with the recycling method used in the DNS. Five different structured, 2D, meshes were built using the open-source platform Salome, in order to ensure a grid-converged solution, and, owing to the relatively low-cost character of the computations, the finest mesh, consisting of 95000 cells, was used for all the computations presented below.

The main effect due to rotation in this type of flows, i.e., the shortening and lengthening of the recirculation bubbles on the anticyclonic and cyclonic sides, respectively, is reproduced by the model. Fig. 7 shows the friction coefficient on the anticyclonic and cyclonic walls. The model reproduces the
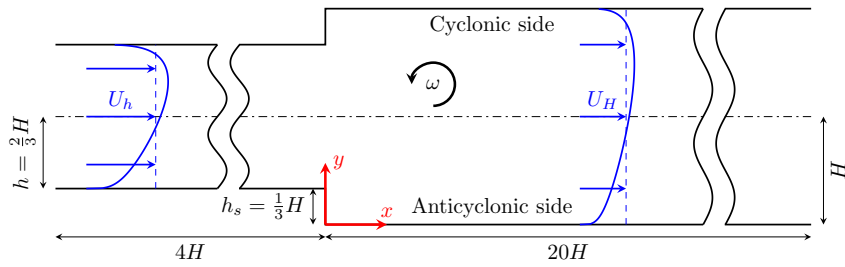
4

Figure 6.   Schematic view of the rotating channel with sudden expansion.

monotonic shortening of the recirculation bubble observed by Rothe & Johnston (1979). For the non-rotating case, the model gives $L_r = 6.80h_s$, which is only 6% above the DNS value and for $Ro = 0.25$, the model shows a 33% reduction of the recirculation bubble, which is to be compared to 31% for the DNS. In contrast, the model is, as already observed in 1D channel flows, over-sensitive to rotation on the cyclonic side. Whereas the DNS exhibits an increase of the recirculation length by a factor 3.1, the model predicts a factor 5.2. Fig. 7a shows that the shape of the C_f distribution on the anticyclonic side, for the non-rotating and the rotating cases, is correctly reproduced. The intensification with the rotation rate of the backflow is predicted, although the intensity is significantly underestimated by the model. After reattachment, the model overestimates the friction coefficient, due to too slow a recovery of the fully developed channel flow profile.

The C_f distributions given by both the DNS and the EB-RSM computation exhibit two additional zero crossings, inside the main recirculation bubble, which are the footprints of secondary and tertiary recirculation bubbles. For the non-rotating case, the extents of these bubbles given by the DNS are $1.9h_s$ and $0.05h_s$, respectively, and $1.2h_s$ and $0.05h_s$ for the model. For the case $Ro = 0.25$, the DNS shows a decrease of the size of the secondary bubble on the anticyclonic side and an increase on the cyclonic side, while the model predicts opposite trends. In contrast, for the tertiary bubble, the model correctly predicts an increase on the anticyclonic side and a decrease on the cyclonic side.

The globally correct predictions of the model on the anticyclonic side, seen in Fig. 7, is confirmed by profiles of the mean velocity shown in Fig. 8. A striking feature is the incorrect deceleration of the flow in the core region ($0.25H < y < 1.25H$) after the reattachment on the anticyclonic side. It clearly appears that this is a side effect of the strong overestimation of the backflow and of the size of the recirculation bubble on the cyclonic side: the negative mass flow rate is overestimated in the cyclonic recirculation region, and does not change sign after the location where DNS predicts the reattachment, such that, in order to preserve the global mass flow rate, the mean streamwise velocity is overestimated in the core region.

Fig. 9 compares the normal Reynolds stress profiles in the non-rotating and rotating cases. It is first observed that the Reynolds stresses are very satisfactory in the incoming channel. After the expansion, on the anticyclonic side, the anisotropy is globally very well reproduced, in particular in the recovery region. However, in the lower half of the core region ($0.25H < y < 0.75H$), the Reynolds stresses go too rapidly to zero: this is to be traced to the above-mentioned misprediction of the streamwise velocity in this region. Indeed, the overestimated recirculation length on the cyclonic side is at the origin of a significant underestimation of the deceleration in the core region. A deceleration yields a transfer of energy from the mean

flow to turbulence through the production term $-\overline{u^2}\partial U/\partial x$ in the $\overline{u^2}$-equation, which helps maintaining the turbulent energy level. Although the DNS Reynolds stress budgets are not available, it can be thus conjectured that the underestimated deceleration is the main reason for the low level of $\overline{u^2}$ in the EB-RSM computation. Due to the pressure and Coriolis redistributions of energy among the components, $\overline{v^2}$ and $\overline{w^2}$ are in turn affected by this mechanism.

CONCLUSION

EB-RSM predictions in the case of a channel with sudden expansion are globally very satisfactory, in particular for the cases without or with anticyclonic rotation, yielding an excellent reproduction of the recirculation length. However, consistent with the rotating channel case, the cyclonic region is found over-sensitive to rotational effects, leading to an overestimation of the recirculation length. This misprediction has a significant impact on the rest of the domain, in particular the core region, which experiences an overestimation of the mean streamwise velocity to compensate for the loss of flow rate on the cyclonic side. Since additional corrections of the model, via the dissipation equation, used in rotating homogeneous turbulence in order to inhibit the energy cascade, were found detrimental to the prediction of the cyclonic side in rotating channel flows, the improvement of the sensitivity to rotation in this region remains an open issue.

REFERENCES

Archambeau, F., Méchitoua, N. & Sakiz, M. 2004 Code Saturne: A Finite Volume Code for the Computation of Turbulent Incompressible flows - Industrial Applications. *Int. J. on Finite Volume, Electronical edition: http://averoes.math.univ-paris13.fr/html* **ISSN 1634** (0655).

Bardina, J., Ferziger, J.H. & Rogallo, R.S. 1985 Effect of rotation on isotropic turbulence: computation and modelling. *J. Fluid Mech.* **154**, 321–336.

Bardina, J., Ferziger, J. H. & Reynolds, W. C. 1983 Improved turbulence models based on large-eddy simulation of homogeneous, incompressible, turbulent flows. Report TF-19. Stanford University, California, USA.

Barri, M. & Andersson, H.I. 2010 Turbulent flow over a backward-facing step. Part 1. Effects of anti-cyclonic system rotation. *J. Fluid Mech.* **665**, 382–417.

Grundestam, O., Wallin, S. & Johansson, A.V. 2008 Direct numerical simulations of rotating turbulent channel flow. *J. Fluid Mech.* **598**, 177–199.

Hallbäck, M. & Johansson, A. V. 1993 Modelling of Rotation Effects in the ε-equation and Reynolds number Influence on slow pressure strain in RST closures. In *Proc. 5th Int. Symp. refined flow modelling and turbulence measurements, 1993*, pp. 65–72.
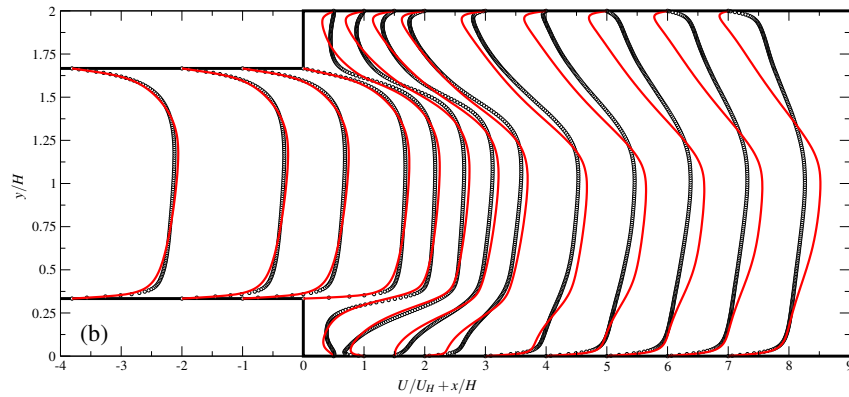
Figure 8.   Rotating channel with sudden expansion. Mean streamwise velocity profiles.
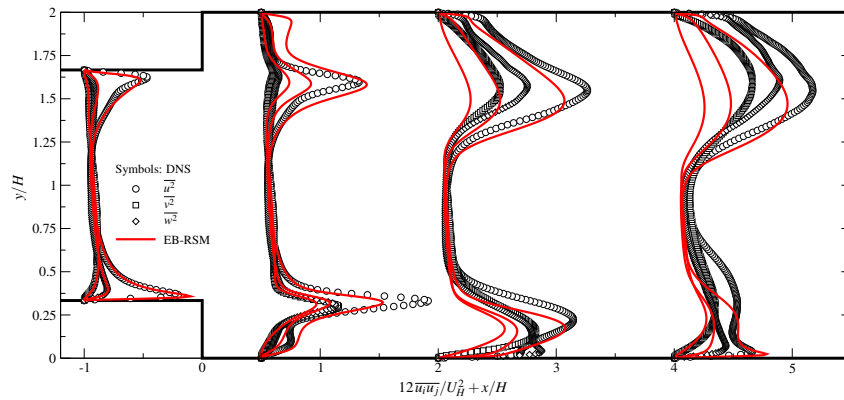

Figure 9.   Rotating channel with sudden expansion. Normal stress ($\overline{u^2}$, $\overline{v^2}$, $\overline{w^2}$) profiles.

Hanjalić, K. & Launder, B.E. 2011 *Modelling Turbulence in Engineering and the Environment. Second-Moment Routes to Closure*. Cambridge University Press.

Iaccarino, G., Ooi, A., Pettersson Reif, B. A. & Durbin, P. 1999 RANS simulations of rotating flows. In *Ann. Res. Briefs*, pp. 257–266. Center for Turbulence Research, Stanford University, CA, USA.

Jacquin, L., Leuchter, O., Cambon, C. & Mathieu, J. 1990 Homogeneous turbulence in the presence of rotation. *J. Fluid Mech.* **220**, 1–52.

Jakirlić, S., Hanjalić, K. & Tropea, C. 2002 Modeling rotating and swirling turbulent flows: A perpetual challenge. *AIAA J.* **40** (10), 1984–1996.

Lamballais, E. 2014 Direct numerical simulation of a turbulent flow in a rotating channel with a sudden expansion. *J. Fluid Mech.* **745**, 92–131.

Lamballais, E., Métais, O. & Lesieur, M. 1998 Spectral-Dynamic Model for Large-Eddy Simulations of Turbulent Rotating Channel Flow. *Theor. Comput. Fluid Dyn.* **12**, 149–177.

Lecocq, Y., Manceau, R., Bournaud, S. & Brizzi, L.-E. 2008 Modelling of the turbulent heat fluxes in natural, forced and mixed convection regimes. In *Proc. 7th ERCOFTAC Int. Symp. on Eng. Turb. Modelling and Measurements, Limassol, Cyprus*.

Lozano-Durán, A. & Jiménez, J. 2014 Effect of the computational domain on direct simulations of turbulent channels up to $Re_\tau = 4200$. *Phys. Fluids* **26** (1).

Manceau, R. 2003 Accounting for wall-induced Reynolds stress anisotropy in Explicit Algebraic Stress Models. In *Proc. 3rd Symp. Turb. Shear Flow Phenomena, Sendai, Japan*.

Manceau, R. 2015 Recent progress in the development of the Elliptic Blending Reynolds-stress model. *Int. J. Heat Fluid Fl.* **51**, 195–220.

Manceau, R. & Hanjalić, K. 2002 Elliptic Blending Model: A New Near-Wall Reynolds-Stress Turbulence Closure. *Phys. Fluids* **14** (2), 744–754.

Mansour, N. N., Kim, J. & Moin, P. 1988 Reynolds-stress and dissipation-rate budgets in a turbulent channel flow. *J. Fluid Mech.* **194**, 15–44.

Rothe, P.H. & Johnston, J.P. 1979 Free shear layer behavior in rotating systems. *J. Fluid Eng.-T. ASME* **101**, 117–120.

Rubinstein, R. & Zhou, Y. 1997 The Dissipation Rate Transport Equation and Subgrid-Scale Models in Rotating Turbulence. ICASE Report 97-63. NASA.

Sagaut, P. & Cambon, C. 2008 *Homogeneous Turbulence Dynamics*. Cambridge University Press.

Shimomura, Y. 1993 *Near-Wall Turbulent Flows*, chap. Turbulence Modeling Suggested by System Rotation, pp. 115–123. Elsevier Science, New York.

Speziale, C. G., Sarkar, S. & Gatski, T. B. 1991 Modeling the pressure-strain correlation of turbulence: an invariant dynamical system approach. *J. Fluid Mech.* **227**, 245–272.

Törnblom, O. & Johansson, A. V 2007 A Reynolds stress closure description of separation control with vortex generators in a plane asymmetric diffuser. *Phys. Fluids* **19** (115108).

Visscher, J. & Andersson, H.I. 2011 Particle image velocimetry measurements of massively separated turbulent flows with rotation. *Phys. Fluids* **23** (7).

Viswanathan, A.K. & Tafti, D.K. 2007 Capturing effects of rotation in sudden expansion channels using detached eddy simulation. *AIAA J.* **45** (8), 2100–2102.